Journal of Hazardous Materials 193 (2011) 304–310

Contents lists available at ScienceDirect

Journal of Hazardous Materials

journal homepage: www.elsevier.com/locate/jhazmat

Tail-end Hg capture on Au/carbon-monolith regenerable sorbents

M. Teresa Izquierdo[a,*], Diego Ballestero[b], Roberto Juan[a], Enrique García-Díez[a,b], Begoña Rubio[a], Carmen Ruiz[a], M. Rosa Pino[b]

[a] Instituto de Carboquímica, ICB-CSIC, c/Miguel Luesma, 4, 50018 Zaragoza, Spain
[b] Instituto de Medioambiente, Universidad San Jorge, Autovía A23 Zaragoza-Huesca km 510, Villanueva de Gállego, 50830 Zaragoza, Spain

ARTICLE INFO

Article history:
Received 4 April 2011
Received in revised form 14 July 2011
Accepted 16 July 2011
Available online 6 August 2011

Keywords:
Hg capture
Regenerable sorbent
Au/C sorbent

ABSTRACT

In this work, a regenerable sorbent for Hg retention based on carbon supported Au nanoparticles has been developed and tested. Honeycomb structures were chosen in order to avoid pressure drop and particle entrainment in a fixed bed. Carbon-based supports were selected in order to easily modify the surface chemistry to favour the Au dispersion. Results of Hg retention and regeneration were obtained in a bench scale experimental installation working at high space velocities (for sorbent, 53,000 h^{-1}; for active phase, 2.6×10^8 h^{-1}), 120 °C for retention temperature and Hg inlet concentration of 23 ppbv.

Gold nanoparticles were shown to be the active phase for mercury capture through an amalgamating mechanism. The mercury captured by the spent sorbent can be easily released to be disposed or reused. Mercury evolution from spent sorbents was followed by TPD experiments showing that the sorbent can be regenerated at temperatures as low as 220 °C.

1. Introduction

The largest anthropogenic source of mercury to the atmosphere in the world is the burning of fossil fuels, primarily coal. Electrical power plants are estimated to account for about 25% of the global anthropogenic mercury emissions to the atmosphere and industrial and residential heating for another 20% [1].

In 2005 the USA Environmental Protection Agency (EPA) established "The Clean Air Mercury Rule" turning the United States into the first country to regulate these emissions. On the other hand, the European Commission published in 2005 the "Community Strategy Concerning Mercury", which identifies coal combustion as one of the main sources of anthropogenic mercury also in Europe. According to the European Environmental Agency (EEA), Spain is the third country among EU27 in mercury emissions, mainly due to coal-fired plants [2].

Mercury is found in coal in the form of sulphides or associated to them, interchanged on clays and associated to the organic matter in low rank coals. During the combustion processes, these forms evaporate, giving rise to Hg(0), HgO and $HgCl_2$, whose proportions in gas phase depend on the concentration and mode of occurrence in the coal and on the compounds present in the gaseous stream, especially particulates and HCl [3]. In some cases, more than 90% of the Hg in coal can be emitted in gas phase through the stack.

Mercury can be removed from coal before combustion by coal cleaning, during combustion depending on unburned carbon, by existing air pollution control devices and with mercury specific control devices. Particulate matter control by ESP or FF controls only particle-bound mercury and FGD units can only remove oxidized mercury. So, specific control processes for elemental mercury capture are now under research or demonstration.

The state of the art technology that has shown promise for controlling element as well as oxidized mercury is active carbon injection (ACI). A major problem associated with ACI technology is that the commercial value of fly ash is sacrificed due to its mixing with contaminated activated carbon powder. So, a system with two separate powder collectors and ACI between the first collector for fly ash and the second collector for activated carbon powder would be necessary. The forthcoming regulation concerning to Hg emissions in the UE and the limited residue production to be accomplished by any depuration technology, make the development of new processes mandatory.

In addition, carbon filter beds present problems associated to the lower affinity between non-treated carbons (without specific active sites) and elemental mercury [4,5] as well as pressure drop in the fixed bed. High efficiency sulphur doped carbons are used for Hg retention on fixed beds, but the problem of toxic wastes still remains.

Regenerable sorbents can accomplish high mercury retention that can be recovered as well as balance cost because of its regenerability. Recognizing reversible characteristics of mercury amalgamate with gold and silver, gold- or silver-coated silica beds have been widely used to pre-concentrate low concentration of

* Corresponding author. Tel.: +34 976 733977; fax: +34 976 733318.
E-mail address: mizq@icb.csic.es (M.T. Izquierdo).

0304-3894/$ – see front matter © 2011 Elsevier B.V. All rights reserved.
doi:10.1016/j.jhazmat.2011.07.065

elemental mercury for its detection [6,7]. The gold– or silver–mercury amalgam is extremely stable at room temperature. However, the amalgam decomposes to release mercury to a gas phase at higher temperatures, leaving clean gold or silver surfaces ready for further mercury capture [7]. In order to effectively collect trace amounts of mercury, it is necessary to have the gold and/or silver in a form of large surface areas [8]. The gold and silver as monolayer is effective for mercury capture [9]. The challenge with this design is that with repetitive exposure to flue gases and heating, the coated gold or silver layer tends to aggregate into larger islands in micrometer sizes, which could lead to inefficient mercury capture [7,8,10].

Despite the preconceived idea concerning Au gold price, it is a little less expensive than Pt, a very common catalyst used in several applications as fuel cells where Pt is used at high concentration. Moreover, it is expected that the spent Au/C sorbent after several cycles of Hg retention–regeneration can be burned to recover gold, improving the economy of the process.

Some tests of Hg capture and sorbent regeneration are found in the literature [7,11]. However, both studies performed mercury adsorption at room temperatures much lower than coal-fired power plant flue gas temperatures or stack temperatures.

In this work, a study of Hg retention and regeneration on Au-based sorbents has been carried out. Au nanoparticles were deposited onto structured carbon monoliths by two different methodologies. These methodologies allow us to reach different Au concentrations on the sorbent surface and different Au particle sizes in order to initially screen the influence of these parameters on the Hg capture efficiency, as a preliminary study before to extend the research to flue gas real conditions.

The novelty of this work is focused on two aspects: the deposition of gold nanoparticles on carbon material, as it is stated in [12] and the Au/C sorbent regenerability study after Hg retention, in order to achieve a waste free process (except Hg itself) for Hg capture.

2. Experimental

2.1. Regenerable sorbents

Honeycomb structured carbon monoliths were used as supports for Au/C sorbents. Raw support (labelled MC-orig) has square channel with a density 69 cell/cm^2.

Different treatments were applied to the raw support in order to modify the surface chemistry to improve further dispersion of gold nanoparticles. Raw supports were oxidized with either nitric acid (labelled MC-HNO3) or air (labelled MC-air). Raw supports were also steam activated (labelled MC-vapor). These procedures are described elsewhere [13].

Two different methods for gold deposition onto the supports have been used: colloidal method and salt method. In colloidal gold method (based on [14]), citrate anion acts as reducing agent of the gold salt and protector of the gold sol formed preventing its aggregation. The second method consists of the direct reduction of a gold salt by the own carbon material of the support (patent under processing). In both methods it is necessary to force the gold suspension/solution to pass through the channels of the monolithic support to achieve a homogeneous gold deposition along the channels of the monolithic supports.

After gold deposition, a reducing treatment was applied to the sorbents. A gas mixture containing 4% H_2/Ar was passed through the sorbent at 300 °C during 1 h. Samples coming from gold salt deposition were labelled adding to the support label -Au-SHC (for sorbent with high Au content on the surface) and -Au-SMC (for sorbent with medium Au content on the surface). Samples coming from the colloidal method were labelled adding to the support label -Au-C2.

2.2. Sorbent characterization

Before gold deposition, supports were characterized by elemental analysis, N_2 physisorption and thermal programmed desorption (TPD). After gold deposition, sorbents were characterized by scanning electron microscopy with energy-dispersive X-ray analyzing system (SEM–EDX), field emission SEM (FE-SEM) and N_2 physisorption.

Surface areas were determined with N_2 at 77 K. The Brunauer–Emmett–Teller (BET) equation was applied to N_2 adsorption isotherms. Prior each analysis, samples were outgassed at 150 °C and up to a vacuum less than 10^{-5} mm Hg.

The TPD runs were carried out with a custom built set-up, consisting of a tubular quartz reactor placed inside an electrical furnace. TPD experiments were carried out by heating the samples up to 1100 °C in Ar flow at a heating rate of 10 °C/min, recording the CO and CO_2 evolved at each temperature with a quadrupole mass spectrometer from Pfeiffer. The calibrations for CO and CO_2 were carried out by standards diluted in Ar. In a typical run 0.5 g of carbon was placed in a horizontal quartz tube reactor under an Ar stream of 30 ml/min.

The study of the gold distribution along the monolith channels was carried out by SEM and the particle size distribution was determined by image analysis from electron micrographs obtained from FE-SEM.

2.3. Mercury retention experiments

A bench scale installation (Fig. 1) was used to determine the sorbent efficiency for the capture of elemental mercury and the maximum retention capacity. This installation consists of flowmeters for nitrogen, a permeation tube for Hg(0) flow generation (inside a tube immersed in a thermostatic bath), a quartz reactor heated by a furnace and an on-line elemental mercury analyzer (VM3000). Moreover, the installation is provided with a tail-end train of flasks to allow the capture of mercury as well as its speciation (in the case of evidence of oxidation under the experimental conditions). The installation is built up with Teflon pipes and pieces (in the part of the installation where Hg is present) to prevent possible mercury attack to steel.

The Hg breakthrough curves were obtained at space velocity 53,000 h^{-1} (considering the whole sorbent, and 2.6×10^8 h^{-1} considering the active phase), 120 °C (near the stack temperature) and Hg inlet concentration of 200 $\mu g/m^3$ (23 ppbv). The Hg(0) total amount retained was calculated from the integration of the breakthrough curve. Some experiments were repeated to test reproducibility. Moreover, some Hg exhausted sorbents were analyzed in a mercury analyzer (AMA) in order to corroborate results on Hg retention from integration of breakthrough curves.

In order to test the best regeneration temperature, Hg temperature programmed desorption (Hg-TPD) of exhausted sorbents was performed on some selected samples. In order to evaluate the appropriate conditions for sorbent regeneration, mercury exhausted sorbent was heated up to 450 °C with a heating rate of 10 °C/min, and the Hg evolution was followed on line as a function of the temperature.

3. Results and discussion

3.1. Support characterization

Table 1 summarizes the results from support characterization. As it can be observed from elemental analysis, the level for intro-

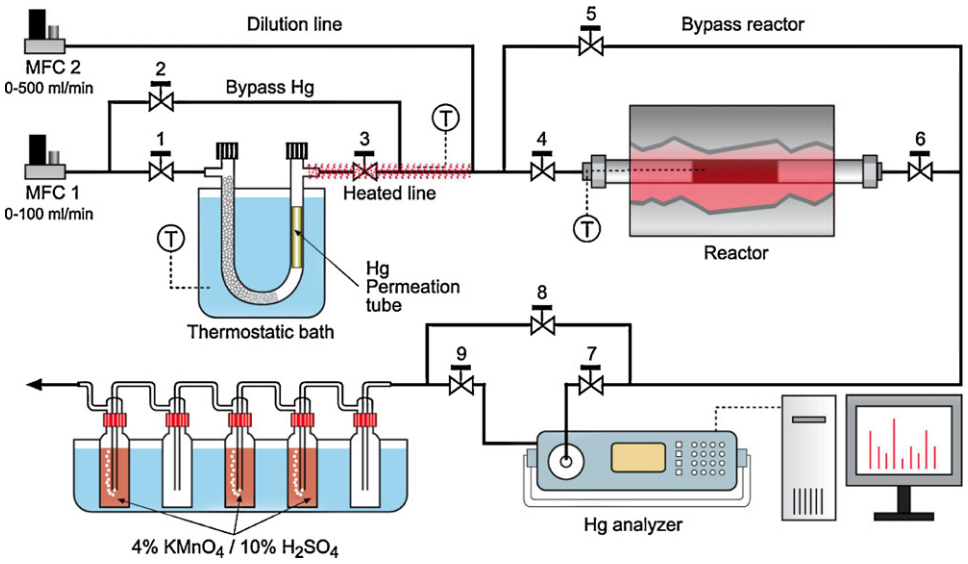

Fig. 1. Experimental installation for Hg retention tests.

duction of oxygen in the raw support structure (MC-orig) is similar for acid-oxidation and steam activation treatments and lower for air-oxidation.

As it can be deduced from Table 1, supports are mainly microporous. Steam activation develops the porous structure of the monoliths with surface area and pore volume being higher than those measured for raw support. Air oxidation of raw support does not alter significantly porous structure and surface area. However, acid oxidation alters the support porosity, decreasing the surface area as well as the total pore volume. It is generally reported that the liquid phase oxidation does not change significantly the texture of the activated carbons, although under more drastic conditions (concentrated acid, heating until complete evaporation) a decrease in the surface and pore volume has been observed [15] due to the collapse of pore walls.

The conditions used to oxidize the raw support change the amount and type of surface oxygen functional groups present on the resulting supports. The amounts of CO and CO_2 desorbed and the temperatures at which these gases released have been found to be characteristics of various oxygen functional groups. It has been proposed that CO_2 derives from functional groups like carboxylic acids, anhydrides and lactones and CO derives from functional groups like phenolic and quinonic groups. Groups yielding CO_2 have been shown to decompose typically over a range of temperatures 150–600 °C while groups yielding CO decompose at temperatures in the range of 600–1000 °C [16].

The total amount of CO and CO_2 evolved up to 1100 °C in a TPD run for each activated carbon is reported in Table 1. As it can be deduced, the three treatments (nitric acid, air or steam) increase the amount of total oxygen groups present in the supports. The introduction of CO-evolving groups is similar for the three supports; however, the introduction of CO_2-evolving groups is much higher for support MC-HNO3. This fact is important to be considered, because it is reported that the deposition of some metals on carbon supports, in particular gold, seems to be favoured by carboxylic-type surface groups [17].

Table 1
Characteristics of the supports.

	MC-orig	MC-HNO3	MC-air	MC-vapor
Elemental analysis				
C (%)	93.86	68.40	88.16	74.66
H (%)	0.80	1.53	0.82	1.49
N (%)	0.25	1.36	0.00	0.19
S (%)	0.00	0.00	0.00	0.00
O (%, by diff)	5.09	28.71	11.02	23.66
N_2 physisorption				
S_{BET} (m^2/g)	430	343	433	750
V_{meso} (cm^3/g)[a]	0.008	0.006	0.011	0.035
V_p (cm^3/g)[b]	0.251	0.204	0.253	0.448
TPD experiments				
CO_2 (mmol/g)	0.313	3.923	0.583	1.054
CO (mmol/g)	1.187	2.821	2.628	2.212

[a] Applying BJH method.
[b] Total pore volume at $p/p_0 = 0.995$.

3.2. Sorbent characterization

Sorbent surface area does not vary significantly after gold deposition, as can be seen comparing surface area values of supports and sorbents in Tables 1 and 2. This fact is indicative of non-pore blockage due to Au nanoparticle deposition.

The study of the distribution of gold along the monolith channels was carried out by SEM–EDX. Monoliths were longitudinal sectioned in order to determine the Au distribution along the channels. Appropriate homogeneity of Au content was found and no Au accumulation in the interaction of the channel and the wall of the monoliths was found. Table 2 shows the Au content on the surface for the sorbents. X-ray photoelectron spectroscopy (XPS) confirmed that Au is in the metallic state and oxidized forms were not detected. It is important to note that the Au content reported in Table 2 is referred to Au surface content not to Au bulk content. The content of Au on the bulk sorbent was determined by ICP-OES and it was 0.11% for sorbent MC-orig-Au-SHC. Little research can be found in the literature concerning Hg capture by regenerable sorbents, some of them concerning Ag as active phase for Hg to be amalgamated. However in those research works [18,19], the Ag content (on bulk sorbent) was at least one order of magnitude higher than that used in this work (for sorbent with the highest amount of Au on the carbon surface).

Micrographs of the sorbents taken by FE-SEM in backscattering mode are shown in Fig. 2. The images show, except for sorbent MC-orig-Au-SHC, that the particles are well separated and dispersed. The surface covered by Au, the Au particle size distribution, the Au Feret average diameter as well as the circularity of the Au particles were obtained using Image Analysis software. Results of this

Table 2
Characteristics of the sorbents.

Sorbent	S_{BET} (m^2/g)	Au (SEM–EDX) (%)	Au surface coverage (%)	Au average particle size (nm)	Au particle average circularity
MC-orig-Au-C2	427	0.83 ± 0.20	4.5	21	0.90
MC-HNO3-Au-C2	n.d.	1.82 ± 0.49	19.4	25	0.86
MC-air-Au-C2	n.d.	0.81 ± 0.22	3.7	19	0.90
MC-vapor-Au-C2	n.d.	1.62 ± 0.47	8.6	20	0.88
MC-orig-SHC	413	8.92 ± 1.18	63.5	–	–
MC-orig-SMC	421	1.94 ± 0.64	26.7	33	0.84

n.d., not determined.

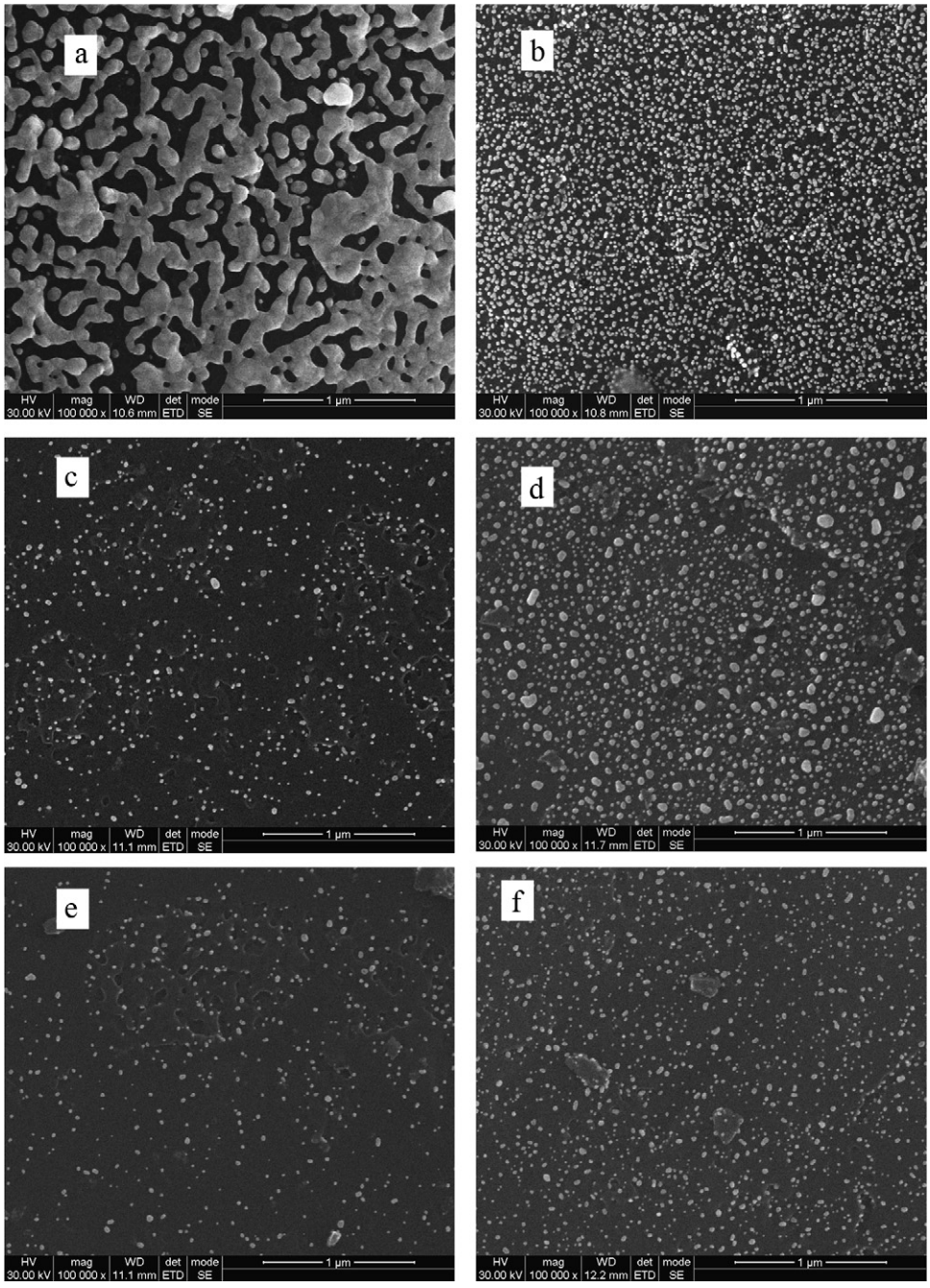

Fig. 2. Fe-SEM micrographs of the sorbents, Au particle size distribution and circularity of the Au particles: (a) MC-orig-Au-HC; (b) MC-orig-Au-SMC; (c) MC-orig-Au-C2; (d) MC-HNO3-Au-C2; (e) MC-air-Au-C2; (f) MC-vapor-Au-C2.

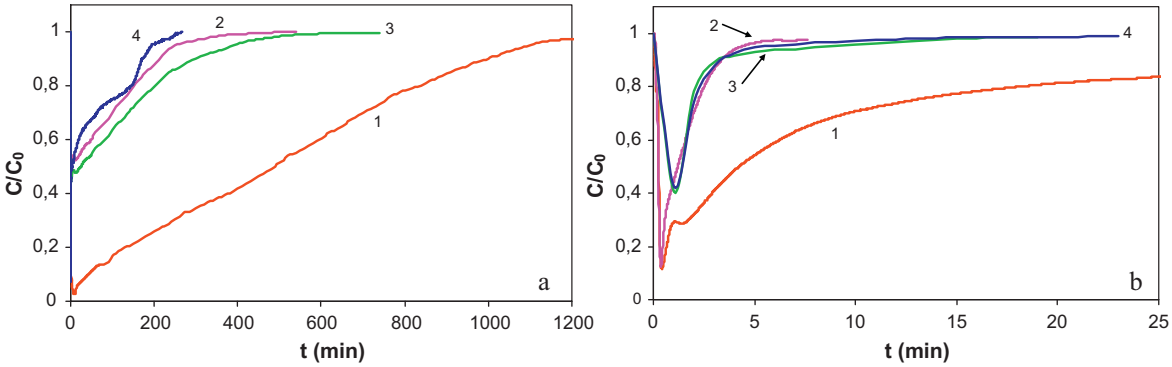

Fig. 3. Mercury breakthrough curves for the supports. (a) 1: MC-HNO3; 2: MC-vapor; 3: MC-air; 4: MC-orig. (b) 1: MC-HNO3-red; 2: MC-vapor-red; 3: MC-air-red; 4: MC-orig-red.

analysis are reported in Table 2. For sorbent MC-orig-Au-SHC only the fraction of surface covered by gold can be obtained; as it can be seen in Fig. 2, Au particles are agglomerated, creating big and connected clusters, making impossible to calculate the particle diameter.

With the sodium citrate method to disperse Au nanoparticles onto the monoliths, the negatively charged citrate ions are adsorbed onto the gold nanoparticles, introducing the surface charge that repels the particles and prevent them from aggregating. However, with the salt method there is a spontaneous gold particle formation onto the carbon material due to the reduction potential of the own carbon material to reduce Au(III). However, particle nucleation on carbon material is fast and ceases in a very short time, after which particle growth, rather than further nucleation, dominates. Therefore, the process needs a fine control to prevent the formation of gold aggregates. These two mechanisms can explain the differences in surface coverage as well as Au particle size reported in Table 2.

There is a straightforward correlation between Au surface coverage and the Au particle diameter, indicating the tendency of Au particles to be sintered when particles are close enough. The amount of Au loaded on the support surface has a big influence on the Au particle diameter. When the surface fraction covered by Au is too high, the size of particle increases and this fact favours the sintering of the Au particles, reaching the formation of big clusters in the case of sorbent MC-orig-Au-SHC. However, there is not a direct correlation between the Au content on the surface and the particle size or surface coverage, but the trend is the higher the Au content on the surface of the support, the higher the Au particle size and surface coverage.

3.3. Mercury retention–regeneration tests

Blank experiments on the supports were carried out in order to test their influence on the retention capacity of the Au-based sorbents. These experiments were performed according to the conditions described in Section 2.

Fig. 3a depicts breakthrough curves for supports and the amount of Hg captured (from integration of the breakthrough curves, when reached 95% saturation, deducting death volume of the reactor) is given in Table 3. As it can be seen, all the supports have some ability for Hg retention, in particular, the support treated with nitric acid, MC-HNO3. However, these supports cannot be considered for real blank experiments. The reason is that once Au is deposited, a reducing treatment is applied to the sorbents, so the real blank is a support that undergoes the same reducing treatment. Thus, reduced supports (labelled as -red) at the same reducing conditions than those undergone by the sorbents were tested for Hg retention capacity.

Fig. 3b depicts Hg breakthrough curves for reduced supports and the amount of Hg captured is given in Table 3. As it can be seen, the saturation time is in the range of few minutes and the amount of Hg captured is negligible, except for support MC-HNO3-red. The behaviour of the support treated with nitric acid (as prepared and reduced) can be explained in terms of surface chemistry of this support. As it can be deduced from Table 1, this support has incorporated a high amount of CO_2-evolving groups, which could chemisorb Hg. Once the support has been reduced, part of these groups disappears and less active sites for Hg chemisorption are available. However, after reduction, this support presents still some Hg retention capacity (higher than the other reduced supports). This fact can be explained in terms of the temperature during reduction treatment. The reduction of support MC-HNO3 was carried out at 300 °C and the appropriate temperature to remove most of the CO_2-evolving groups is around 400 °C. In order to check this hypothesis, MC-HNO3 exhausted support was subjected to a TPD to follow the evolution of the Hg adsorbed onto the support. Fig. 4 shows the Hg-TPD curve in which two peaks can be observed. First peak appears at 220 °C and can be attributed to Hg retained through physisorption mechanism. Second peak appears at 430 °C and can be attributed to Hg retained through chemisorption mechanism onto CO_2-evolving groups, which are removed completely near 550 °C. Once the Hg has been removed from support MC-HNO3, a breakthrough curve for Hg was obtained for the regenerated support (MC-HNO3-reg), resulting in a negligible retention of Hg, since Table 3, obtaining similar values of Hg retention capacity than those obtained for the rest of the supports once reduced.

These results agree with those reported in the literature concerning with the low affinity between non-treated activated

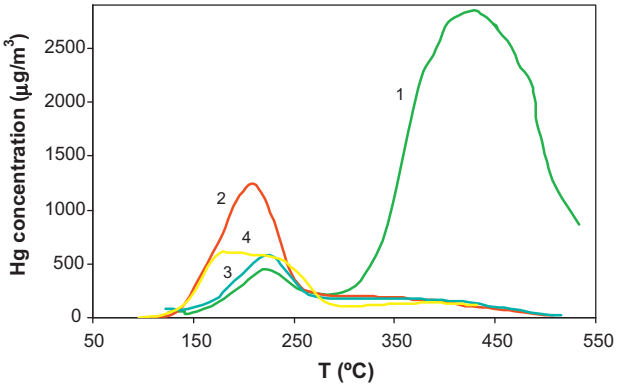

Fig. 4. Measured outlet Hg concentration in temperature programmed desorption for exhausted support (1: MC-HNO3) and for exhausted sorbents (2: MC-orig-Au-SHC; 3: MC-orig-Au-SMC; 4: MC-HNO3-Au-C2).

Table 3
Total amount of Hg captured by the supports and the sorbents.

Support	Hg captured[a] (μg/g support)	Hg captured[b] (μg/g support)	Sorbent	Hg captured[a] (μg/g sorbent)	Efficiency[c] (%)
MC-orig	9.94		MC-orig-Au-SHC-1	29.7	88.9
MC-HNO3	87.86	81.69	MC-orig-Au-SHC-2	29.0	89.0
MC-vapor	26.40		MC-orig-Au-SMC	10.8	78.0
MC-air	12.19		MC-orig-Au-C2	5.7	78.3
MC-orig-red	0.26		MC-HNO3-Au-C2	10.1	76.1
MC-HNO3-red	2.62		MC-air-Au-C2	6.0	75.1
MC-vapor-red	0.58		MC-vapor-Au-C2	12.1	75.6
MC-air-red	0.24				
MC-HNO3-reg	0.39				

[a] From integration of breakthrough curves up to 95% saturation.
[b] Direct determination on the exhausted support by mercury analyzer (AMA).
[c] From integration of breakthrough curves up to 30% saturation and the amount of Hg feeded up to the time corresponding to 30% saturation.

carbons (without specific active sites) and elemental mercury [4,5]. Both studies conclude that heterogeneous oxidation with subsequent binding on the surface is needed to retain the Hg. In the case of treated carbon sorbents, mercury retention is predicted to occur entirely by chemisorption.

Fig. 5 depicts the breakthrough curves for the Au/C sorbents and Table 3 summarizes the total amount of Hg retained on the sorbents (calculated from the integration of the breakthrough curves, when reached 95% saturation, deducting death volume of the reactor and the contribution of the supports). First noticeable observation is the reproducibility of the experiments, taking into account that the inlet Hg concentration is as low as 23 ppbv (200 $\mu g/m^3$). Because the on-line mercury analyzer only determines the concentration of elemental mercury present in the gas, in some of the duplicated experiments the possible oxidation of elemental mercury by Au catalytic oxidation was followed. The train of flasks containing a chilled solution of $KMnO_4/H_2SO_4$ and chilled solution of KCl was placed after the mercury analyzer in order to retain elemental and oxidized mercury, respectively (the so-called Ontario-Hydro ASTM method). Both solutions were further analyzed by cold-vapor atomic absorption. No oxidized mercury was detected in any of the flasks analyzed. Thus, all the mercury is in the form of Hg(0) that can amalgamate. However, the presence of SO_2 and NO in the flue gas could contribute to catalyze mercury oxidation in the presence of Au nanoparticles; so ongoing work is being carried out on this topic.

Because the time needed to reach the same level of saturation is different for each sorbent, Table 3 also reports the efficiency of Hg retention calculated as the ratio between the amount of Hg retained by the sorbents at 30% of saturation and the total amount of Hg feeded into the reaction during this time. The value of 30% of saturation was chosen considering that in real application the saturation or near-saturation of the sorbents is never reached.

The distinct difference in mercury capture by the supports and the sorbents demonstrates the decisive role of Au nanoparticles deposited onto the carbon monoliths for mercury capture. Thus, it can be said that the mercury capture on the Au/C sorbents is based on the amalgam mechanism. Similar findings are reported in the literature with Au or Ag supported on other carbon materials [20].

As it can be deduced from Table 3 there is not a direct relationship between Au content and either Hg capture capacity of the sorbents at the same level of saturation or capture efficiency. This fact means that not all the Au deposited on the supports is efficient for Hg capture. There are overwhelming evidence concerning the size dependence on chemical reactivity. Smaller particles have large number of atoms at the surface [21–23]. These atoms differ from atoms in the bulk of the crystal in the way that they have an incomplete set of nearest neighbours (i.e. coordination number). Thus, a small Au nanocrystal of 1 nm diameter would have nearly 100% of its atoms on the surface and at increasing diameter the amount of atoms on the surface would be decreased. Although those studies were related to catalytic applications of Au nanoparticles, some work can be found related to the influence of the Au surface morphology at the nanometer scale and the role of active sites on Hg/Au amalgam formation [24].

According to those findings, in the present case the Au nanoparticles size has a big influence on the Hg capture efficiency, as it can be seen in Fig. 6. Despite not being possible to calculate Au particle size of sorbent MC-orig-Au-SHC, its efficiency for mercury retention has been added into this figure, out of scale, only for comparison purpose. It is clearly seemed that there is a compromise between

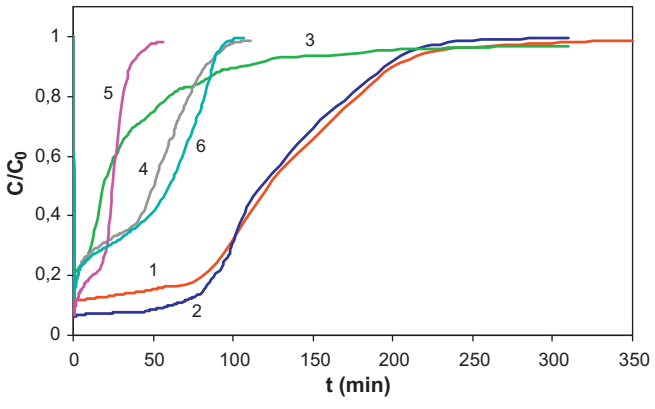

Fig. 5. Mercury breakthrough curves for the sorbents. 1: MC-orig-Au-SHC-1; 2: MC-orig-Au-SHC-2; 3: MC-orig-Au-SMC; 4: MC-HNO3-Au-C2; 5: MC-orig-Au-C2; 6: MC-vapor-C2.

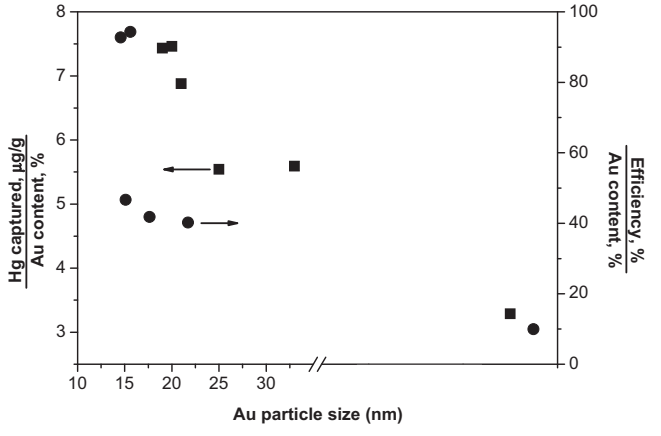

Fig. 6. Relationship between Hg captured by the sorbents and the amount of Au and its particle size (amount of Hg captured at 95% saturation; efficiency at 30% saturation).

the Au amount on the surface and the particle size reached. So, efforts have to be focused on the development of a sorbent with higher Au content on the carbon surface and an appropriate Au particle size.

Exhausted sorbents were subjected to a Hg-TPD to follow the evolution of the Hg adsorbed onto the sorbents in order to study the release temperature for mercury amalgamated in order to obtain the appropriate temperature for sorbent regeneration. Fig. 4 shows Hg-TPD curves for some sorbents. The captured mercury started to release at 100 °C, reaching the maximum around 220 °C. At 275 °C, approximately the 90% of the captured mercury has been evolved. These results suggest that the appropriate temperature for sorbent regeneration is slightly higher than 200 °C. This temperature is lower than that used to prepare the sorbent as described in Section 2. This fact leads to consider that under this temperature and atmosphere the nanoparticles are not expected to undergo sintering. However, the removal of mercury from the gold crystal lattice could affect the point defects of the lattice [23] and thus the following step of mercury capture onto the regenerated sorbent. This aspect should be carefully studied, but in this case we are limited by the amount of Au deposited (0.1% in the best case), which conditions the available techniques to study the regenerated sorbents because of their detection limits.

The mechanism for Hg retention onto the sorbents is different from that showed for support MC-HNO3 as it can be deduced from Fig. 4. The chemisorption mechanism is very limited after removing CO_2-evolving groups (sorbents have all been reduced at 300 °C in H_2 atmosphere) from supports, as it can be deduced from the total amount of Hg captured given in Table 3. So, the mechanism for Hg retention could be attributable to the amalgamation with Au nanoparticles also for sample MC-HNO3-Au-C2. This fact is very significant, because temperatures for sorbent regeneration are lower than those for support MC-HNO3 and do not depend on the surface chemistry of the sorbents. However, a small tail for mercury evolution is found at higher temperature, suggesting that some mercury is still retained on the sorbent; this fact could be indicative of some Hg chemisorption on the support, corresponding to the activity exhibited by supports and reported in Table 3. In order to completely remove all the Hg from the sorbents, regeneration temperature should be increased, reducing the advantage of the economy of low temperature regeneration. On the other hand, the non-released mercury should be a constant along capture–regeneration cycles and this fact should not modify Hg capture after the first regeneration cycle. Further work will be directed to investigate this hypothesis.

4. Conclusions

Regenerable sorbents based on Au deposition on structured carbon-based monoliths have been developed and tested to determine their Hg capture capacity as well as their regenerability. Sorbents with Au bulk content lower than 0.1% can retain nearly 30 mg Hg/g Au, exhibiting a high efficiency for mercury capture. However, the Hg capture capacity of sorbents is not directly related to the amount of Au supported. The most important factor determining elemental mercury retention seems to be the gold nanoparticle size and a balance between the amount of Au supported and the nanoparticle size should be found.

The regeneration of the Hg exhausted sorbent can be carried out at low temperature if the absence of CO_2-evolving groups (from TPD) is guaranteed, in order to avoid Hg chemisorption on carbon support.

Acknowledgements

The financial support from Spanish Ministry of Science and Innovation (ref: CTQ2008-06860-C02-02/PPQ) is duly recognized. Authors want to thank Susana Cortés for CVAA mercury analysis.

References

[1] The Global Atmospheric Mercury Assessment: Sources, Emissions and Transport, UNEP Chemical Branch, UNEP-Chemicals, Geneva, 2008.
[2] European Union emission inventory report 1990–2008 under the UNECE Convention on Long-range Transboundary Air Pollution (LRTAP), EEA Technical Report 7/2010, Copenhagen, 2010.
[3] E.S. Olson, B.A. Mibeck, Oxidation kinetics and the model for mercury capture on carbon in flue gas, in: International Conference on Air Quality V, Arlington, VA, September 19–21, 2005.
[4] F.E. Huggins, N. Yapa, G.P. Hyffman, C.L. Senior, XAFS characterization of mercury captured from combustion gases on sorbents at low temperature, Fuel Process. Technol. 82 (2003) 167–196.
[5] B. Padak, J. Wilcox, Understanding mercury binding on activated carbon, Carbon 47 (2009) 2855–2864.
[6] S.J. Long, D.R. Scott, R.J. Thompson, Atomic absorption determination of elemental mercury collected from ambient air on silver wool, Anal. Chem. 45 (1973) 2227–2233.
[7] R. Nowakowski, T. Kobiela, Z. Wolfram, R. Duoes, Atomic force microscopy of Au/Hg alloy formation on thin Au films, Appl. Surf. Sci. 115 (1997) 217–231.
[8] F.H. Schaedlich, D.R. Schneeberger, Cartridge for collection of a sample by adsorption onto a solid surface, U.S. Patent 5,660,795 (1997).
[9] M. Levlin, E. Ikävalko, T. Laitinen, Adsorption of mercury on gold and silver surfaces, J. Anal. Chem. 365 (1999) 577–586.
[10] C. Battistoni, E. Bemporad, A. Galdikas, S. Kaciulis, G. Mattogno, S. Mickevicius, V. Olevano, Interaction of mercury vapour with thin films of gold, Appl. Surf. Sci. 103 (1996) 107–111.
[11] T.Y. Yan, A novel process for Hg removal from gases, Ind. Eng. Chem. Res. 33 (1994) 3010–3014.
[12] Highlights from recent literature, Gold Bull. 43 (2010) 66–74.
[13] R. Juan, M.T. Izquierdo, C. Ruiz, B. Rubio, Preparation and characterization of carbon-based regenerable sorbents for mercury retention, in: Carbon'2009, International Conference on Carbon, Biarritz, France, 2009.
[14] J. Turkevich, P.C. Stevenson, J. Hillier, A study of the nucleation and growth processes in the synthesis of colloidal gold, Discuss. Faraday Soc. 11 (1951) 55–75.
[15] J.S. Noh, J.A. Schwarz, Effect of HNO_3 treatment on the surface-acidity of activated carbons, Carbon 28 (1990) 675–682.
[16] R.C. Bansal, J.B. Donnet, F. Stoeckli, Active Carbon, Marcel Dekker, New York, 1988.
[17] L. Jiang, L. Gao, Modified carbon nanotubes: an effective way to selective attachment of gold nanoparticles, Carbon 41 (2003) 2923–2929.
[18] Y. Liu, D.J.A. Kelly, H. Yang, C.C.H. Lin, S.M. Kuznicki, Z. Xu, Novel regenerable sorbent for mercury capture form flue gases of coal-fired power plant, Environ. Sci. Technol. 42 (2008) 6205–6210.
[19] J. Dong, Z. Xu, S.M. Kuznicki, Mercury removal from flue gases by novel regenerable magnetic nanocomposite sorbents, Environ. Sci. Technol. 43 (2009) 3266–3271.
[20] G. Luo, H. Yao, M. Xu, X. Cui, W. Chen, R. Gupta, Z.Z. Xu, Carbon nanotube–silver composite for mercury capture and analysis, Energy Fuels 24 (2010) 419–426.
[21] M. Haruta, Size- and support-dependency in catalysis of gold, Catal. Today 36 (1997) 153–166.
[22] M. Haruta, Gold as a novel catalyst in the 21st century: preparation, working mechanism and applications, Gold Bull. 37 (2004) 27–36.
[23] S. Schimpf, M. Lucas, C. Mohr, U. Rodemerck, A. Bruckner, J. Radnik, H. Hofmeister, P. Claus, Supported gold nanoparticles: in-depth catalyst characterization and application in hydrogenation and oxidation reactions, Catal. Today 72 (2002) 63–78.
[24] R. Nowakowski, T. Kobiela, Z. Wolfram, R. Dus, Atomic force microscopy of Au/Hg alloy formation on thin Au films, Appl. Surf. Sci. 115 (1997) 217–231.